MULTI-CAVITY FIELD EMISSION AT STF-2 ACCELERATOR IN KEK

P. Joshi*[1], T. Matsumoto[1,2], S. Michizono[1,2], Y. Yamamoto[1,2], T. Oyama[1,2]
[1]SOKENDAI (The Graduate University for Advanced Studies), 240-0193, Hayama, Japan
[2]KEK (High Energy Accelerator Research Organization), 305-0801, Tsukuba, Japan

Abstract

In December 2022, an experiment was conducted in an STF-2 accelerator to measure neutron and gamma radiation levels both upstream and downstream by tuning eight cavities with an average gradient of 31 MV/m. The model was evaluated to understand the measured data. In this model, the electrons generated by field emission (FE) are accelerated through multiple cavities applied and discussed. The key finding emphasized the dominance of multi-cavity FE over a single cavity based on the FE number, FE point, self-cavity loss, adjacent cavity loss, tune loss, and detune loss according to the tuning and detuning of the cavity.

INTRODUCTION

The superconducting RF test facility (STF) of the High Energy Accelerator Research Organization (KEK) is a facility for the R&D of the technologies of the International Linear Collider (ILC) main linacs [1]. These include R&D in radio frequency (RF) production, RF distribution, superconducting (SC) cavities, and cryomodules. The STF-2 L-band photocathode RF gun serves as an injector for the two SC cavities in a capture cryomodule, eight SC cavities in CM-1, and four SC cavities in CM-2a [2]. The RF power for the 12 SC cavities is generated using a 10 MW pulsed multibeam klystron (CETD Co. Ltd, E3736H) [3]. Different models of the local power distribution systems developed at STF are installed in STF-2. Table 1 summarizes the operational parameters of the STF-2 accelerator.

Table 1: STF-2 Accelerator Operational Parameters in 2022

Parameters	Value and Unit
Operational frequency	1.3 GHz
Accelerating mode	TM_{010}, π-mode
Average gradient	31 MV/m
RF pulse width	1.65 ms
Pulse repetition rate	5 Hz
Beam energy	≈400 MeV
Bunch spacing	6.15 ns
Bunch charge	35.7 pC
Bunch current	5.8 mA
Operational temperature	2 K

Field emission (FE) plays a major role in the degradation of SC cavity performance [4]. The effect of the FE on the performance of the cavity can be understood from the relationship between the quality factor, X-ray, and accelerating gradient [5]. When several cavities are operated, identifying the contribution of FE by each cavity becomes more complex. Therefore, a model is considered to understand the FE of an individual cavity (CAV#) and its contribution to the total FE during the multi-cavity operation.

* prakashj@post.kek.jp

EXPERIMENT

Four cavities of CM-1 and four cavities of CM-2a were used in the experiment of FE. To measure the radiation, a neutron counter and gamma detector were placed downstream and upstream, respectively, as shown in Fig. 1. The gate valves on both sides remained closed, and the SC quadrupole magnet between CAV#4 and #5 was shut down during the experiments. The radiation level on the downstream side was measured as the average accelerating gradient of the eight cavities increased from 18 MV/m to 31.5 MV/m. Furthermore, the radiation level was measured on both sides by tuning and detuning the individual cavities, maintaining an average gradient of 31 MV/m.

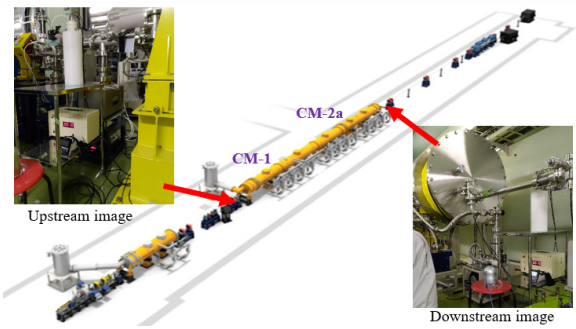

Figure 1: Position of the neutron counter and gamma detector in the schematic of the STF-2 accelerator.

MEASUREMENT

In Figs. 2 and 3, the dark blue colored bar shows the radiation detected when all the cavities were tuned, and the green colored bar shows the radiation level when the cavity was detuned. The fluctuations in the blue bar indicate probable statistical and instrumental errors.

Downstream

When CAV#12 was detuned, FE decreased significantly, whereas on detuning CAV#11, FE also decreased significantly. The magnitude increased gradually on detuning cavities from #12 to #8, as shown in Fig. 2. The magnitude of radiation is the sloped line from the detuning of CAV#12, #11, #10, #9, and #8 to all tuned cavities, as shown in Fig. 2. The magnitude of gamma radiation is approximately four times that of neutrons, as shown in Fig. 2. The radiation

level remained the same for the detuning CAV#1, #2, and #5, as shown in Fig. 2.

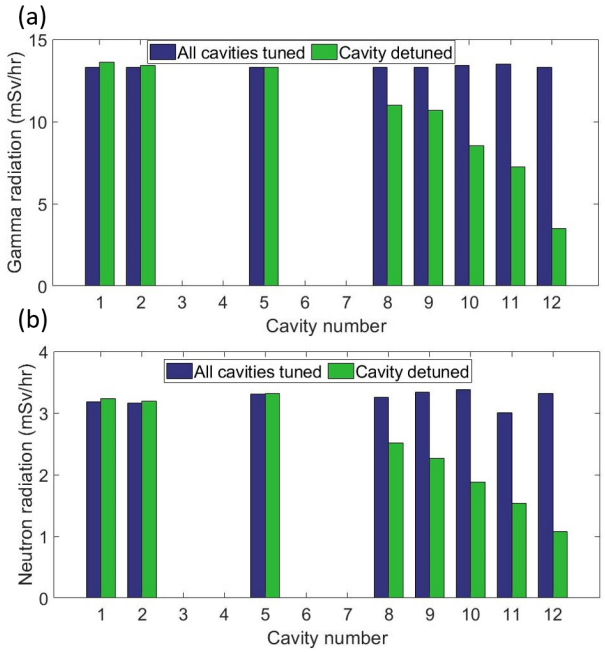

Figure 2: (a) Measured data of gamma radiation downstream when cavities were tuned and detuned individually. (b) Measured data of neutron radiation downstream when cavities were tuned and detuned individually.

Upstream

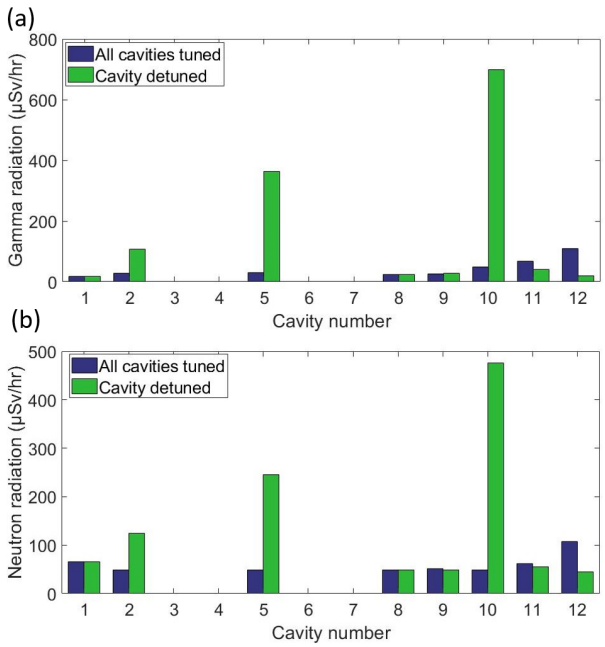

Figure 3: (a) Measured data of gamma radiation upstream when cavities were tuned and detuned individually. (b) Measured data of neutron radiation upstream when cavities were tuned and detuned individually.

The magnitude of radiation on the upstream side was minimal compared to that on the downstream side. Upon detuning CAV#10, the radiation level is significantly higher than those of the others, as shown in Fig. 3. In addition, there was a high FE for detuning CAV#5. The difference in the gamma and neutron radiation levels is small, as shown in Fig. 3.

Single Cavity

Table 2 shows the FE for single cavity operation when a detector is placed just below each cavity. The cavity gradient during the multi-cavity operation is listed in Table 2.

Table 2: X-ray Dose below each Cavity during Single Cavity Operation [6]

Cavity	Gradient (MV/m)	X-ray (μSv/hr)
1	29.0	20
2	31.0	180
5	35.0	820
8	30.9	5,540
9	33.4	3,480
10	30.9	340
11	29.8	90
12	28.2	7,000

ANALYSIS OF MEASUREMENT

The data is analyzed based on the following assumptions: First, the FE number, FE point, self-cavity loss, and adjacent-cavity loss are distinct for each cavity, upstream and downstream. The tune loss is the same for all tuned cavities, and the detune loss is the same for all detuned cavities. Here the FE number is the assumed number of emitted electrons from a cavity, and the FE point is the assumed most probable point of FE, whose value ranges from 0 to 1, as shown in Fig. 4. The self-cavity loss is the fraction of electrons lost inside the field-emitting cavity, whereas the adjacent cavity loss is the fraction of electrons lost in the neighboring cavity. The tune loss is the fraction of electrons lost in a tuned cavity, whereas the detuned loss is the fraction of electrons lost in the detuned cavity. Second, the irises are considered as FE points, as shown in Fig. 4 [7].

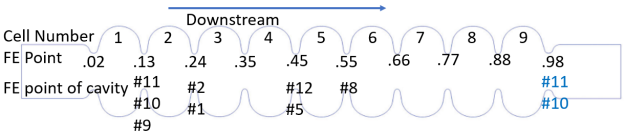

Figure 4: Assumed field emission point for each cavity. Because the dose below CAV#10 and #11 is small, two field emission point is considered.

Third, when electrons are emitted from any cavity, self-cavity loss is applied in the first, adjacent-cavity loss in the second, and tune or detune loss in the third according to

the tuning and detuning of the cavity. The survived electrons are stopped at the gate valve. Finally, the X-ray dose below each cavity is due to FE particles lost inside the cavity.

In general, the phase of the following cavity is delayed relative to that of the previous cavity by +90° ($5.75\lambda_0$=1326 mm) on the downstream side. Therefore, the emitted electrons are either lost by collision with the cavity surface or accelerated downstream, as shown in Fig. 5. The operating cavities are in the decelerating phase on the upstream side, as shown in Fig. 5. However, electrons are accelerated in both directions for CAV#5 and #2 because of the 180-degree phase difference between CAV#4 and #5, as shown in Fig. 6. In upstream, CAV#1 to #8 behaves as detuned cavities for CAV#9 to #12 because of the 45° phase relationship between CAV#8 and #9, as shown in Fig. 6. The spacing between the cavities is shown in Fig. 6.

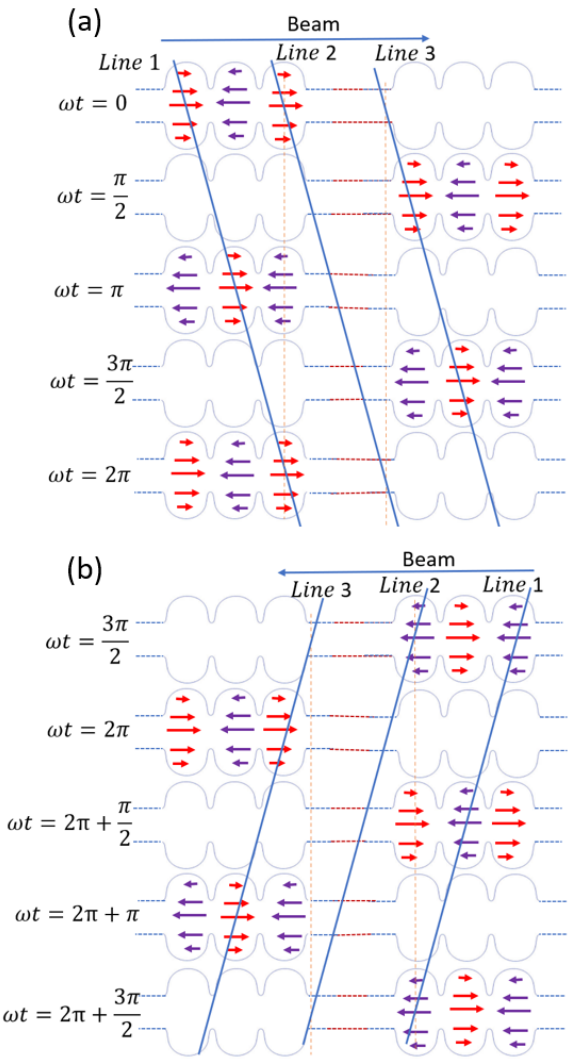

Figure 5: The figures show the variation in the direction of the electric field with time. (a) Acceleration of electrons when moving from Line 1 to Line 3 downstream. (b) Deceleration of electrons when moving from Line 1 to Line 3 upstream.

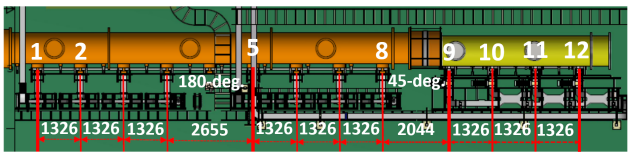

Figure 6: Spacing between the STF-2 cavities. Operated cavities are numbered on the cryomodule and the spacing between cavities is in mm.

There was a loss of electrons in the non-operated cavities, which is referred to as the detune loss. The space between CAV#4 and #5 behaved as a detuned cavity. Furthermore, the radiation level decreased with the square of the distance between the source and the detector.

There were three measured data, including the radiation level on the downstream and upstream sides and the X-ray dose below each cavity. The parameters used to understand multi-cavity FE were considered based on the three measured datasets. The self-cavity loss varies with the emission point, as shown in Fig. 7. The dose produced due to self-cavity loss was optimized using the measured data. The percentages of electrons directed downstream and upstream also differ according to the location of the FE point, as shown in Fig. 7.

In Fig. 7, for emission point A, the self-cavity loss is small with a high adjacent cavity loss, and the electrons are directed upward. At emission point B, the electrons were directed downward, with maximum loss inside the cavity. At emission point C, all FE were trapped inside the cavity.

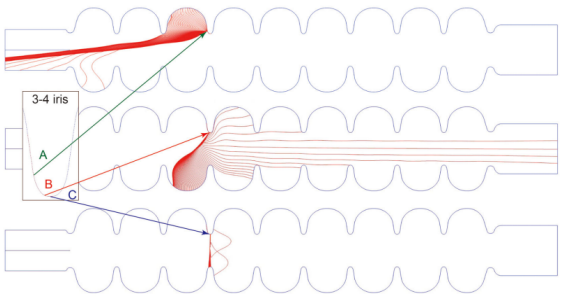

Figure 7: An example illustrating the variation in self-cavity loss and adjacent cavity loss with changes in the emitter point for the same iris located between cells 3 and 4 [8].

The X-ray dose produced by a cavity depends on the number of lost electrons and the energy of the electrons, which can be calculated using the following relations:
Downstream dose ∝ [(1-FE point)*Gradient]*Lost FE number, and Upstream dose ∝ [FE point*Gradient]*Lost FE number, then Dose below a cavity = Downstream dose + Upstream dose. The lost FE number measures different types of losses such as self-cavity loss, adjacent cavity loss, tune loss, and detune loss.

Calculation for Model in case of Cavity 8

Suppose the FE point located on the iris between cells 5 and 6, i.e., 0.55, contributes to the total dose below the CAV#8. The assumed FE number for CAV#8 in downstream is 375, of which 95% are lost in the cavity itself after gaining energy from 4 cells that produce a dose of 4,950 [(1-0.55)*30.9*(375*0.95)], as shown in Fig. 8. Furthermore, 70% of the surviving particles (70% of 19) are lost in the adjacent CAV#9 after gaining energy from 4 cells of CAV#8 and all cells of CAV#9 that produces a dose of 629 [[(1-0.55)*30.9+33.4]*(19*0.70)] when CAV#9 is tuned, as shown in Fig. 8. Furthermore, when CAV#9 is the detuned dose by adjacent cavity loss becomes 185 [[(1-0.55)*30.9]*(19*0.70)]. In the following cavities, either a tune loss of 5% or a detune loss of 10% is applied according to the tuning and detuning of the cavity. The lost particles produce FE, and finally, the surviving particles are stopped at the gate valve, emitting radiation.

(a)

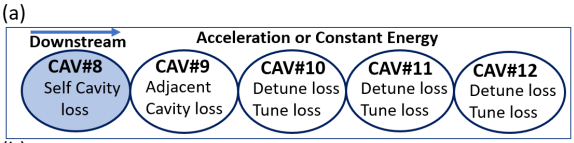

(b)

Downstream	Self-Cavity Loss	Adj. cavity Loss	Tune Loss
Cavity losses	95%	70%	5%
Survived Particles	19	6	5
Dose by lost Particles	4,950	629	22

Figure 8: Schematic of losses in the downstream of cavity-8. (a) Considered types of losses with cavity number. (b) The magnitude of loss and its contribution to field emission.

(a)

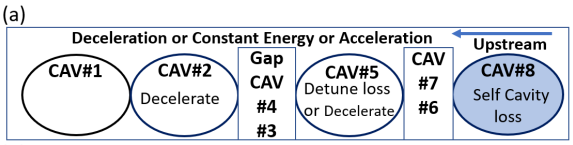

(b)

Upstream	Self-Cavity Loss	Adj. cavity Loss	Tune Loss
Cavity losses	10%	20%	Decelerate
Survived Particles	293	234	0
Dose by lost Particles	552	995	3,580

Figure 9: Schematic of losses in the upstream of cavity-8. (a) Considered types of losses with cavity number. (b) The magnitude of loss and its contribution to field emission.

The assumed FE number for CAV#8 upstream is 325, of which 10% is lost in the cavity itself after gaining energy from five cells that produce a dose of 552 [0.55*30.9*(325*0.10)], as shown in Fig. 9. Furthermore, 20% of the surviving particles (20% of 293) are lost in CAV#7 as an adjacent cavity loss, producing a dose of 995 [0.55*30.9*(293*0.20)], and the survived particles move with the same energy, as shown in Fig. 9. The detune loss is applied in CAV#6, which is a non-operated cavity. If CAV#5 is tuned, all surviving electrons are decelerated by producing a dose of 3,580, as shown in Fig. 9. If CAV#5 is detuned, the electrons travel with the same energy, experiencing detune losses in each cavity and the space between CAV#4 and #5 and decelerate at CAV#2 with the emission of radiation, as shown in Fig. 9.

The cumulative dose, the sum of the upstream and downstream doses, is 5,502 (Figs. 8 and 9), which almost matches the measured data (Table 2) in magnitude. The large number of electrons lost on the downstream side and the small number on the upstream side are determined based on the X-ray dose measured on the upper and lower sides of the operating CAV#8. In the downstream, electrons either move with the same energy and detune loss or accelerate with a tune loss. In the upstream, the electron either moves with a detune loss or decelerates the FE from CAV#8.

COMPARISON

Measured and Modeled Data

The modeled data is optimized based on the measured data of the X-ray dose below each cavity, multi-cavity FE on downstream and upstream, and the assumptions. The violet bars in Fig. 10 show the measured gamma radiation data on the downstream and upstream sides, respectively. The rust color bars in Fig. 10 represent the modeled data on the downstream and upstream sides, respectively.

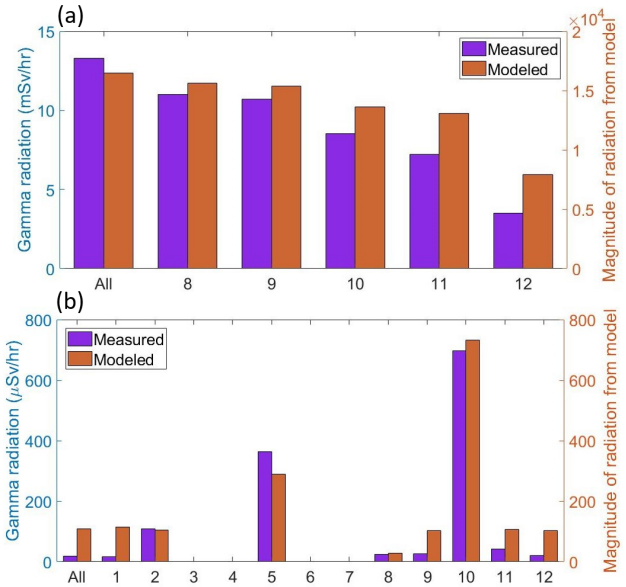

Figure 10: Comparison between measured data and modeled data. (a) Downstream (b) Upstream

The ratio of the measured downstream and upstream data is the same as that of the modeled downstream and upstream data, as shown in Fig. 10. The nature of the graph for modeled and measured data is the same for upstream and downstream, as shown in Fig. 10. The first bars in Fig. 10 show eight cavities tuned cases, and the number on the bar indicates that the cavity is detuned.

Multi-cavity and Single Cavity FE

The FE increases exponentially with an increase in the accelerating gradient in 9 cell SC cavities [9]. CAV#12 is the most contaminated cavity with the lowest accelerating gradient, as shown in Fig. 11. However, CAV#9 exhibits the best performance with a maximum operational accelerating gradient of 36 MV/m and a small FE, as shown in Fig. 11. The measured value of gamma radiation due to multi-cavity FE is approximately twice that of the most contaminated CAV#12. This relationship remains consistent in modeled data. Hence, multi-cavity FE enhances gamma radiation.

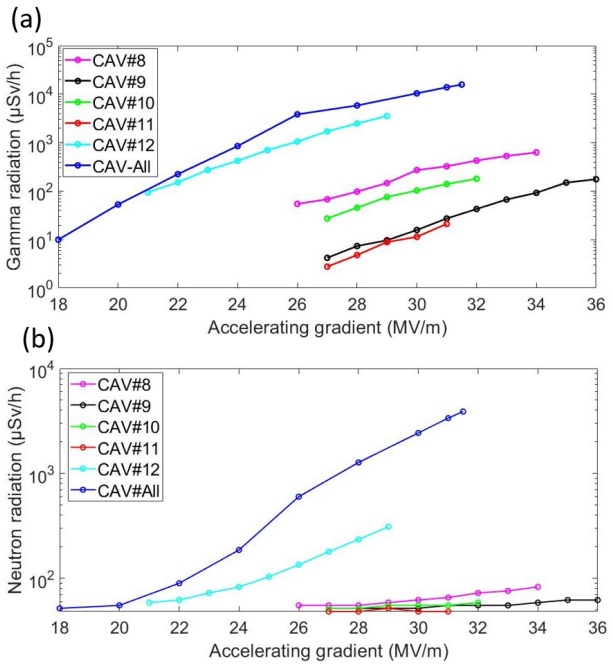

Figure 11: (a) Comparison between the measured data of gamma radiation for single and multi-cavity field emission with increasing accelerating gradient. (b) Comparison between the measured data of neutron radiation for single and multi-cavity field emission with increasing accelerating gradient.

The measured value of the neutron radiation due to the multi-cavity FE is approximately four times the FE due to CAV#12 at an accelerating gradient of 28 MV/m, as shown in Fig. 11. The multi-cavity FE enhances the neutron radiation, which is higher than gamma radiation because energetic electrons striking the metal surface produce neutrons, and the energy of electrons is higher in the multi-cavity FE than in a single cavity. Among the single cavities, the neutron number increases significantly for CAV#12, as shown in Fig. 11. This implies that most of the electrons are accelerated in multiple cells in this cavity.

SUMMARY

The multi-cavity field emission was analyzed using a model based on single-cavity field emission and assumptions. According to the model, the maximum number of electrons was lost in the field-emitting cavity and then in the adjacent cavity, and the loss was small in the following cavity. The surviving electrons were stopped at the gate valve. In the downstream, the survived electrons were accelerated by the succeeding cavities. Therefore, the contribution of the following cavity to the field emission was higher. This was the reason for high field emissions on the downstream side. The radiation level on the upstream side was small owing to the deceleration of electrons in the preceding cavity and small field emission from CAV#1. Furthermore, when CAV#10 was detuned, the field emission from CAV#11 was accelerated in #9 and survived up to the gate valve with a detuning loss in CAV#8 to #1. Thus, the field emission was high. Additionally, the measured data indicated the dominance of multi-cavity field emissions over a single cavity, which matched the modeled data. Finally, a model prepared to understand multi-cavity field emission based on these assumptions almost satisfied the measured data. Thus, the model could explain the phenomenon that occurred inside the superconducting cavity.

ACKNOWLEDGEMENTS

I am thankful to Kazuya Ishimoto, Naoto Numata, and Taiga Hanawa of the NAT group for their help with the experimental setup and measurements.

REFERENCES

[1] ILC, https://linearcollider.org

[2] STF-KEK, https://www2.kek.jp/stf/

[3] https://etd.canon/en/product/category/microwave/klystron.html

[4] B. Bonin, "Field emission in RF cavities", *Atomic Energy Commission, DSM/DAPNIA, France.* https://cds.cern.ch/record/399571/files/p221.pdf

[5] Yasuchika Yamamoto *et al.*, "Achievement of stable beam operation at 36 MV/m in STF-2 Cryomodules at KEK", *18th International Conference on RF Superconductivity, Lanzhou, China, July 2017, pp. 722-728.*

[6] Yasuchika Yamamoto *et al.*, "Report on the operation of STF-2 cryomodule for ILC", *20th Annual Meeting of the Accelerator Society of Japan, Funabashi, Aug. 29 - Sep. 01, 2023, THP58.*

[7] Enrico Cenni, "Field emission study on CW superconducting cavity", *Ph.D. Thesis, Acc. Science Dept., The Graduate University for Advanced Studies, SOKENDAI, Japan, 2013.* https://ir.soken.ac.jp/records/4901

[8] Hiroshi Sakai *et al.*, "Field emission studies in vertical test and during cryomodule operation using precise X-ray mapping system", *Physical Review Accelerators and Beams 22, 022002, 2019.* doi:https://doi.org/10.1103/PhysRevAccelBeams.22.022002

[9] Yasuchika Yamamoto *et al.*, "Stable beam operation at 33 MV/m in STF-2 cryomodule at KEK", *20th International Conference on RF Superconductivity, East Lansing, USA, May 2021, pp. 382-386.*